Microstructure and properties of Cu-rich 123: Part II. Homogeneous copper and high magnetic J_c

J. P. Zhang, D. J. Li, C. Boldt, R. Plass, V. Dravid, and L. D. Marks
Science and Technology Center for Superconductivity, Department of Materials Science and Engineering, Northwestern University, Evanston, Illinois 60208-3108

C. H. Lin and J. A. Eades
Science and Technology Center for Superconductivity, Materials Research Laboratory, University of Illinois at Champaign–Urbana, 104 South Goodwin, Urbana, Illinois 61801

A. Sodonis, W. Wolbach, J. M. Chabala, and R. Levi-Setti
Science and Technology Center for Superconductivity, The Enrico Fermi Institute and Department of Physics, The University of Chicago, Chicago, Illinois 60637

(Received 2 April 1992; accepted 19 January 1993)

Copper- and yttrium-rich $YBa_2Cu_3O_7$ bulk superconductors have been prepared by mixing copper oxide or yttrium oxide in nitric acid and adding the solution to premade stoichiometric $YBa_2Cu_3O_7$ followed by annealing. In contrast to materials made by mixing oxide powders, both samples contain copper-rich defects spread homogeneously throughout the grains, either small platelet copper oxide precipitates or bundles of planar defects (Cu–O double planes). These materials also show large magnetic hysteresis at 77 K, comparable to the results obtained from decomposed $YBa_2Cu_4O_8$. This implies that small copper oxide precipitates and bundles of planar defects are strong flux pinners, and indicates a processing route to producing large amounts of strongly intragranular pinned superconductors. However, the materials also show clean grain boundaries, so an equally valid interpretation is that there is a substantial component of intergranular superconductivity in field, enhancing the effective circuit size to a value far larger than the grain size.

I. INTRODUCTION

Perhaps the most important materials challenge in high temperature superconductors is producing a bulk material with good properties at 77 K. This is in fact two problems: solving the problem of weak links at the grain boundaries and solving the problem of flux pinning within the grains of the material. Although eventually both of these will have to be solved simultaneously, it is easier to approach them one at a time, and our concern herein is with the latter. A very attractive analogy to heterogeneous flux pinning (as against intrinsic, homogeneous flux pinning) within a grain is dispersion strengthening of a material, i.e., use of small second-phase precipitates to reduce flux flow. The type of questions to be answered are what type of precipitates and what morphologies are optimal for flux pinning; this type of information can then be used to try to design a superconductor.

In an earlier paper,[1] we reported in some detail the microstructure and Bean model critical current results of a set of copper-rich samples produced by mixing the elemental oxides and annealing. In these samples the copper was restricted to the grain boundary region, and although there was a small enhancement in J_c at 4.5 K compared to a control sample, at 77 K the results were slightly worse. These results indicated that copper at the grain boundaries alone is not a good flux pinner. In this note, we report results using a different processing technique where the results for both copper- and yttrium-enriched samples are a homogeneous distribution of small copper oxide precipitates and bundled planar defects throughout the grains [which are due to a concentration of 1/3 $(103)^{2-4}$ double copper plane defects]. The magnetic J_c is now strongly enhanced. The data appear to indicate that copper-rich defects of a proper size are strong flux pinners. However, there is an ambiguity in the results since enhanced intergranular transport is an equally viable interpretation.

II. SPECIMEN PREPARATION

Conventional $YBa_2Cu_3O_7$ was mixed with either yttrium oxide or copper oxide dissolved in nitric acid, and the resultant slurry pressed into $1 \times 5 \times (1-4)$ mm pellets after drying at room temperature. The initial compositions of the compounds in this work were $YBa_2Cu_{3+x}O_7$ ($x = 0.5$) or $Y_{1+y}Ba_2Cu_3O_7$ ($y = 0.1$).

The pellets were preheated and annealed in oxygen as follows:

(1) Preheating

$$25\ ^\circ\text{C} \xrightarrow{18\ \text{h}} 900\ ^\circ\text{C} \xrightarrow{4\ \text{h}} 900\ ^\circ\text{C} \xrightarrow{18\ \text{h}} 25\ ^\circ\text{C}$$

(2) Annealing

$$25\ ^\circ\text{C} \xrightarrow{24\ \text{h}} 815\ ^\circ\text{C} \xrightarrow{36\ \text{h}} 815\ ^\circ\text{C} \xrightarrow{1\ \text{h}} 900\ ^\circ\text{C} \xrightarrow{1\ \text{h}} 900\ ^\circ\text{C} \xrightarrow{1\ \text{h}} 815\ ^\circ\text{C} \xrightarrow{3\ \text{h}} 815\ ^\circ\text{C} \xrightarrow{24\ \text{h}} 25\ ^\circ\text{C}$$

III. MAGNETIC AND MICROSTRUCTURE CHARACTERIZATION

We followed the same procedure as used previously to characterize the samples. The magnetic measurements were performed using a Quantum Design Squid at both 4.5 K and 77 K, although we will report only on the latter. The lower resolution microstructure was investigated using samples that were mechanically polished with oil-diluted diamond paste, etched by a 3% bromine solution in ethyl alcohol, and then examined by optical microscopy, SEM, and Secondary Ion Mass Spectroscopy (SIMS) imaging with a high resolution Scanning Ion Microprobe[5] (SIM). The higher resolution microstructure of the crushed powder and ion-beam thinned samples was examined by high resolution electron microscopy (HREM) at 300 kV in a Hitachi H-9000, scanning transmission electron microscopy (STEM) in a VG HB501 and HREM, Convergent Beam Electron Diffraction (CBED), and Nanodiffraction and x-ray microanalysis (EDX) with a Hitachi HF-2000.

IV. RESULTS

For convenience, we will break down the results into a number of sections on the larger scale microstructure, the atomic scale microstructure, and the magnetic properties.

A. Large scale microstructure

The most significant observation regarding the present samples was that, except for the grain boundaries, there were no detectable chemical inhomogeneities. This is illustrated in Fig. 1, which shows evidence for this obtained by high resolution imaging SIMS with the University of Chicago SIM. Since the edge enhancements of the boundary yields due to the grain boundary structure of samples could be misinterpreted as true chemical inhomogeneities, a special procedure was employed to eliminate these edge effect artifacts. This consists of acquiring distribution maps of two elements simultaneously, using a mass peak switching technique.[6] By then dividing one image by the other, true chemical composition distribution can be emphasized, and spurious enhancements erased. Thus, Figs. 1(a) and 1(b) show, respectively, maps for O^- and Cu^- from Cu-rich samples. These images are dominated by the edge enhancements at the grain boundaries. However, the ratio of these images shown in Fig. 1(c) reveals a uniform distribution of Cu relative to O, on a size scale larger than 50 nm. Similarly for the Y-rich samples, SIMS maps for Ba^+ and YO^+ are shown in Figs. 1(d) and 1(e), while their ratio is shown in Fig. 1(f). Once again, no discrete compositional variation in the relative amounts of these constituents can be detected. For reference, it should be pointed out that in our earlier work[1] where the copper phase separated, this was clearly visible in the SIMS maps (see, in particular, Fig. 2 in Ref. 1).

Samples for optical metallography were prepared using mechanical polishing and chemical etching as used for previous Cu-rich samples.[1] The images showed a slightly different morphology from that previously observed, with lines across them as shown in Fig. 2. We believe that these are subgrains due to clusters of copper-rich planar defects (see below) forming subgrain boundaries. The size of these subgrains was around 0.4–0.7 μm. Due to the difficulties in measuring the grain size in these samples, we will use 3 μm as the Bean-model grain size in the "J_c" calculations; from the SIMS maps, this would appear to be a reasonable value.

B. Atomic scale microstructure

From transmission electron micrographs of the material, what was most apparent for both samples was that there were planar defects and/or small precipitates throughout the grains (see Figs. 3 and 4). (In the yttrium-doped material, there were some grains of the green phase Y_2BaCuO_5.) We should note that the planar defects were more common, and the small precipitates comparatively rare.

From the location of the planar defects within the unit cell and the (HREM) image contrast, they could be immediately identified as copper-rich planar defects.[2–4] In addition, x-ray microanalysis and electron energy loss spectroscopy confirmed the determination of these defects as excess CuO.[7] [In HREM images it is relatively simple to isolate the basal plane and the 1/3(301) displacement of the defects. Coupled with careful comparison of the experimental images with numerical simulations both from our own earlier work[2,4] and that of others, it is now well established that these defects are basal copper double planes, similar to local regions of $YBa_2Cu_4O_8$ composition.] Determining the structure of the precipitates was more complicated. Small area nanodiffraction patterns (5–10 nm radius), as shown in Fig. 5, show streaks due to the limited spatial extent of the precipitates and some higher intensity spots which can be indexed in terms of a slightly distorted Cu_2O; presumably the Cu_2O is distorted in order to fit into the

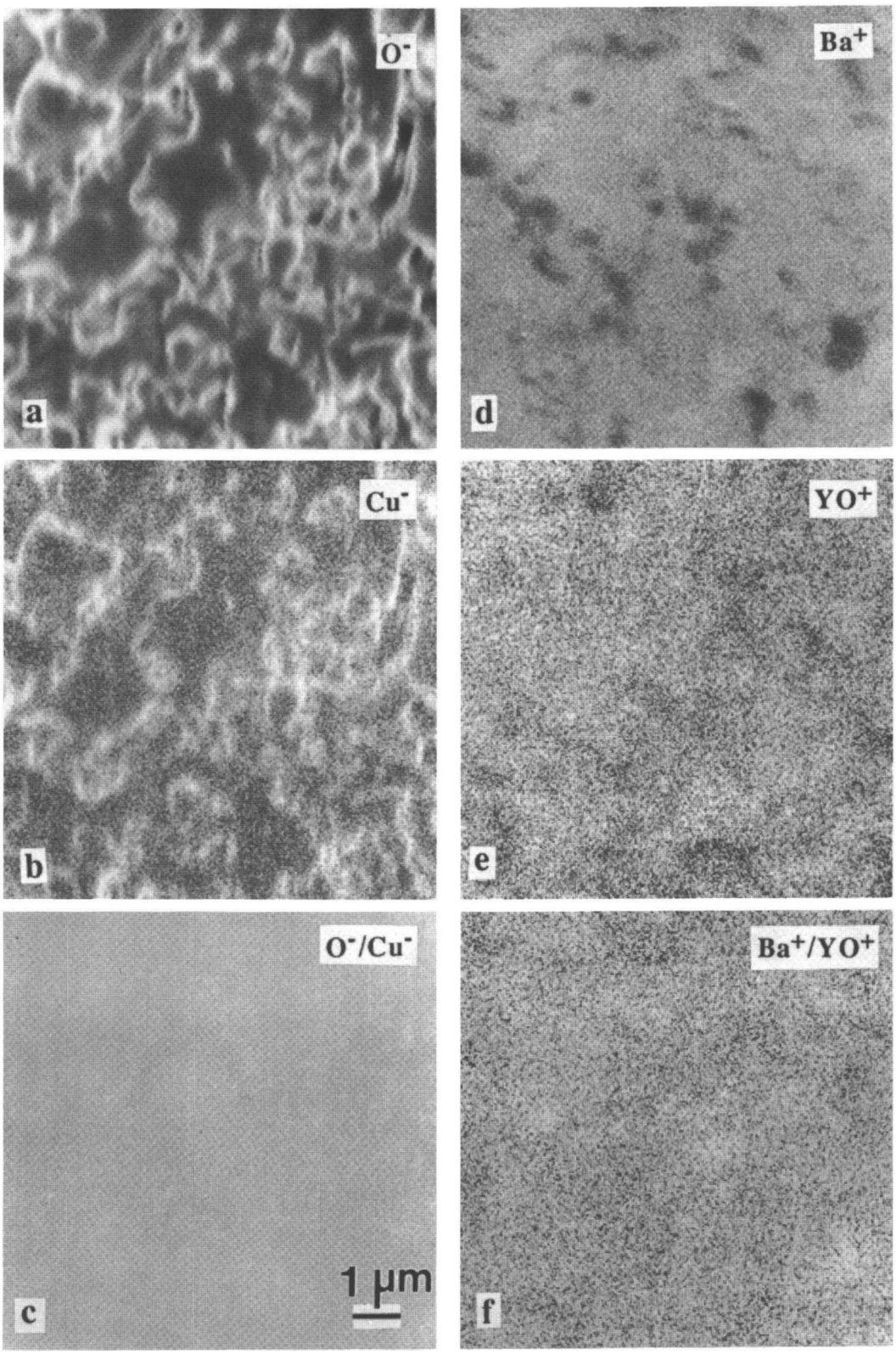

FIG. 1. Pairs of analytical SIMS maps acquired simultaneously by peak switching with the UC SIM and their ratio. This method[6] eliminates artifacts due to edge enhancements of the emission yields. For the Cu-rich sample, O^- and Cu^+ maps are shown in (a) and (b), and the ratio of these images in (c). The texture due to edge effects at grain boundaries disappears in the ratio image, indicating no significant compositional inhomogeneities. For the Y-rich sample, Ba^+ and YO^+ maps are shown in (d) and (e), with (f) the ratio. Again, topographic effects are eliminated in the ratio image, showing a rather uniform relative composition for these two species.

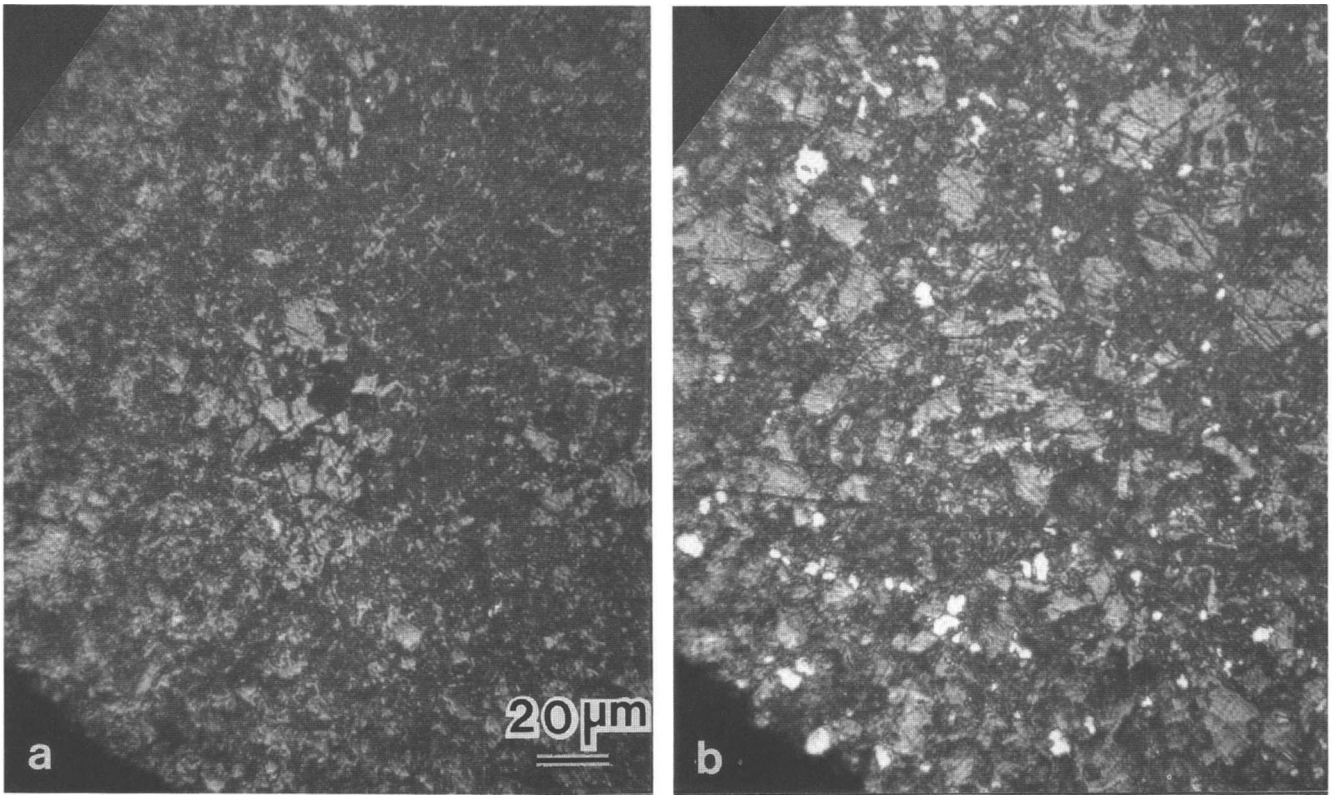

FIG. 2. Optical metallographs of $YBa_2Cu_{3.5}O_7$ in (a) and $Y_{1.1}Ba_2Cu_3O_7$ in (b) showing the fine subgrains due to the presence of clusters of planar defects in the grains.

bulk superconductor matrix. In support of this interpretation, we should mention that these precipitates were located in less defective areas, and that the planar defects in some cases terminated at the precipitates.

Different from the earlier samples,[1] the planar defects were homogeneous throughout the grains, as shown in Figs. 3 and 4. The size of these bundles in the *c*-direction is from 30 Å, a few Cu-rich planar units, to about 0.2 μm. An enlarged image inserted in Fig. 3 shows a typical picture of bundles formed by a few distorted, kinked planar units due to the extra copper. There was no evidence of any congregation near the grain boundaries, and the latter appeared to be quite clean, as shown in Fig. 6.

C. Magnetic properties

Samples for SQUID measurement were bars of size $1 \times 5 \times (1-4)$ mm. These bars were porous with a density of 3.5 to 5.0 g/cm^3, i.e., 55% to 80% dense. A relatively large amount of the samples (about 7 g) was originally produced and measured in two different machines (one at Northwestern and another at Argonne National Labs) with the same results for both. No detectable difference in the measurements was found for different relative orientations of the bars with respect to the magnetic field of the SQUID.

For a polycrystalline sample, it is common to calculate a critical current from the grain size using the Bean model,[8] i.e.,

$$J_c = 30\ \Delta M/r = \alpha \Delta M'$$

where ΔM is the difference in magnetization per unit volume, and r is the radius of the circulating current loop. To reduce the data, we used $2r = 3$ μm, i.e., the grain size as the circulating current loop size, and divided the sample mass by 6.24 g/cm^3 to give the superconducting volume. With $\Delta M'$ in units of emu/g, the value of α is 1.24×10^6. The data are shown in Tables I and II for the excess copper and yttrium samples, respectively, and compared with our earlier data[1] in Table III. (All the data are 77 K.) The Bean values of J_c obtained in this way showed quite high values, comparable with those reported for thermally decomposed 124.[9]

V. DISCUSSION

It certainly appears that when the copper is homogeneously distributed throughout the grains, the magnetic properties of the material are improved. Compared to our earlier work,[1] these samples contain bundles of copper-rich planar defects which are possible flux pinners, stronger than other possible pinners such as point defects

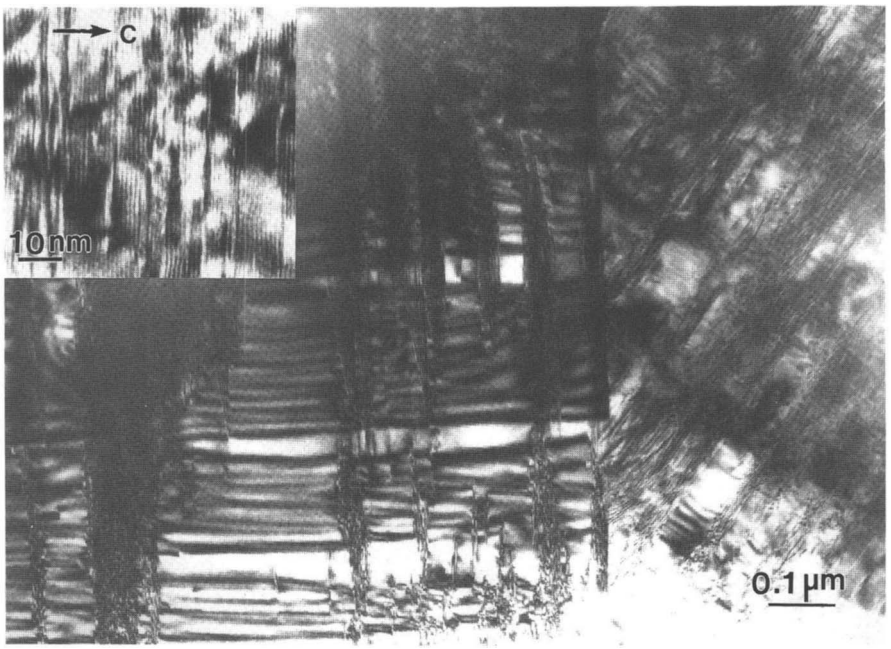

FIG. 3. Images of ion-beam-thinned samples showing bundles of defects (perpendicular to the c-axis), which travel through grains rather than being concentrated at the grain boundaries as observed in lower J_c samples.[1] An enlarged picture inset shows the Cu-rich planar defects in 123 matrix.

or dislocations. An interpretation of the data is that these bundles are pinners. However, there is a major ambiguity here that is also present in reports of enhanced flux pinning in bulk materials.[9,10] The problem is what is the circuit size to be used in a Bean model interpretation of the magnetic results? The standard approach in the literature is to use the grain size, which assumes that the grain boundaries are all nonsuperconducting in

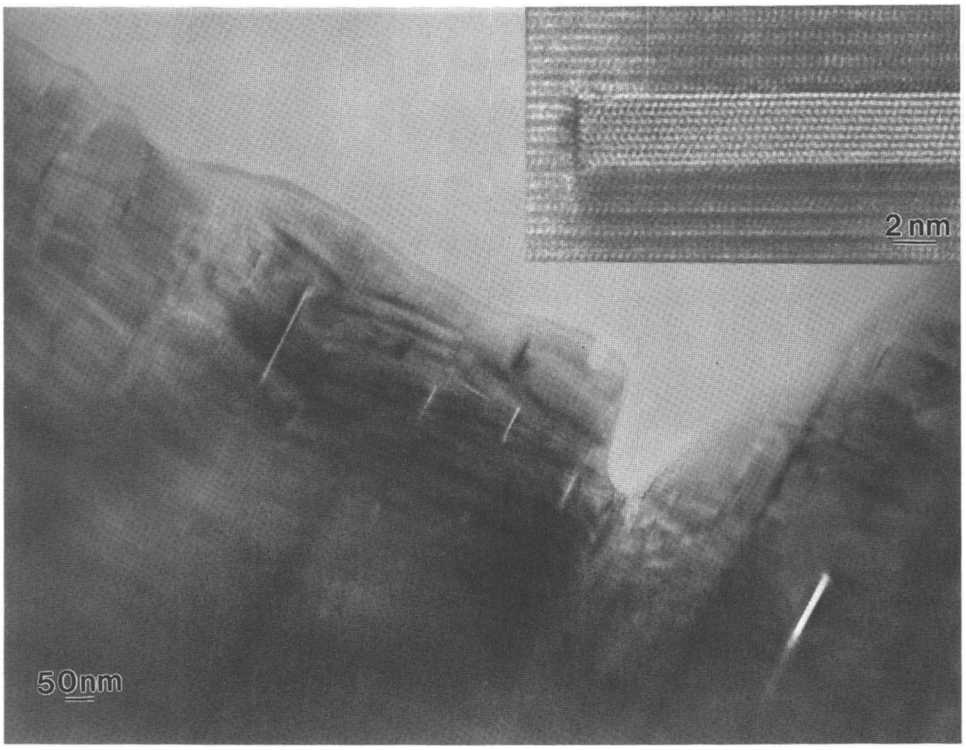

FIG. 4. A low magnification image of the Cu-rich sample showing the precipitates measuring 2–10 nm along the c-axis and 10–100 nm in the a-b plane, which are found (infrequently) in relatively clean areas. Precipitates were observed as well as in the Y-rich samples. The inset is a high resolution image of one of the precipitates.

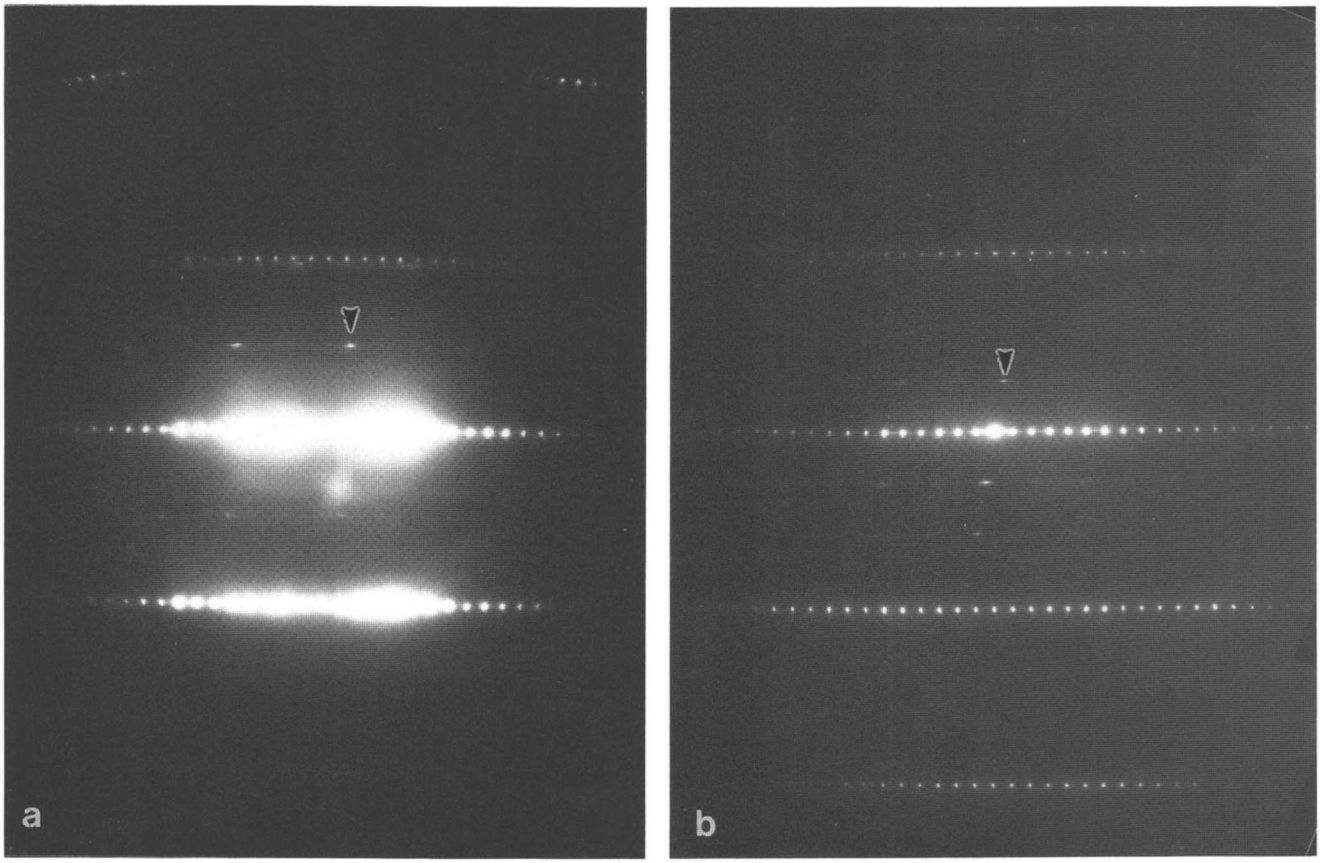

FIG. 5. Nanodiffraction patterns from within one grain of two precipitates found in the Y-rich $YBa_2Cu_3O_7$ samples. The higher intensity spots are the [130] oriented matrix crystal while the weaker spots indicate a Cu_2O type structure for those precipitates with d-spacings of 0.25 nm of Cu_2O {111} and 0.42 nm for {100} for the arrowed spots in (a) and (b), respectively.

any reasonable field. This cannot be correct since bulk ceramic superconductors do carry transport currents in field (albeit typically small values), and there is also now evidence[11] that not all grain boundaries are insulators.

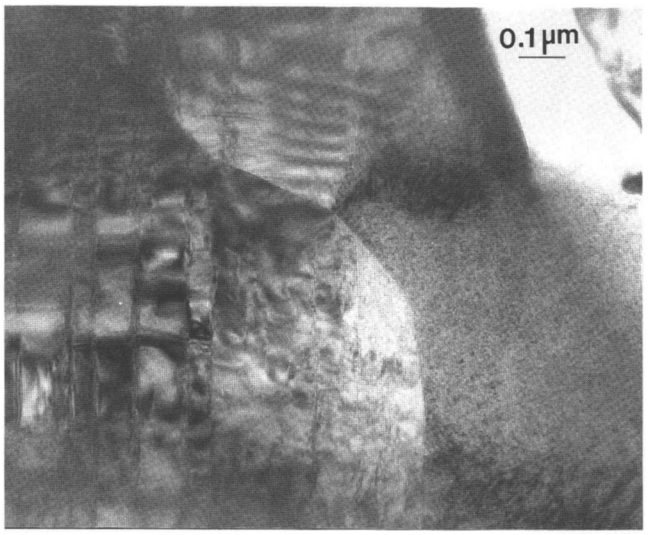

FIG. 6. Typical grain boundaries in the samples.

In the samples described herein, the grain boundaries appear to be quite clean (certainly compared to our previous work), so we cannot rule out some intergranular transport. If, instead of the grain size, we were to take a distribution of circuit sizes, some of which could be large relative to the grain size, the data would not support any flux-pinning effects from the defects. Alternatively, if the grain size is the true circuit size, we have achieved flux pinning to some degree. The drop of the critical current with field is suggestive of weak-link behavior from somewhat conducting grain boundaries, but one could also propose a model with a decrease in effective pinning with increasing field.

This is a genuine ambiguity that we are still working on in attempts to find other experiments that can be more definitive. To date, we have not found any experiment that cleanly proves or disproves either model. For instance, we have looked at thermally decomposed $YBa_2Cu_4O_8$; we see enhanced magnetization, but also clean grain boundaries similar to the work reported herein. We have also tried to reproduce the data with a similar powder sample, but find a very broad T_c which indicates that the penetration length may be perturbing

TABLE I. Magnetization measurement and the calculated J_c of the nitric-acid-treated $YBa_2Cu_{3.5}O_x$ sample (No. 1281).

H (Tesla)	0.00	0.02	0.05	0.10	0.30	0.50	0.70	0.90	1.00	3.00	4.00	5.00	5.50
$-M\nearrow$ (10^{-2} emu/g)	4.085	88.27	106.6	82.99	47.75	39.27	34.65	31.78	30.65	21.06	18.79	17.04	16.29
$-M\swarrow$ (10^{-2} emu/g)	−36.87	−1.128	17.05	27.76	35.98	34.62	32.43	30.53	29.65	20.91	18.70	16.88	···
J_c (A/cm^3)	5.1×10^5	1.1×10^6	1.1×10^6	6.9×10^5	1.5×10^5	5.8×10^4	2.8×10^4	1.6×10^4	1.3×10^4	1.9×10^3	1.2×10^3	2.0×10^3	···

Here the $M\nearrow$ and $M\swarrow$ present the magnetization measured in the fields with positive and negative increments, respectively.
Sample No. 1281: size $\sim 1 \times 5 \times 2.62$ mm; mass $m = 0.0601$ g.

TABLE II. Magnetization measurement and the calculated J_c of the nitric-acid-treated $Y_{1.1}Ba_2Cu_3O_x$ sample (No. 1293).

H (Tesla)	0.00	0.02	0.05	0.10	0.30	0.50	0.70	0.90	1.00	3.00	4.00	5.00	5.50
$-M\nearrow$ (10^{-2} emu/g)	8.609	147.5	132.8	83.16	48.10	38.92	34.62	31.52	30.26	19.58	16.77	14.66	13.71
$-M\swarrow$ (10^{-2} emu/g)	−62.18	4.836	22.77	32.47	38.81	36.01	33.01	33.56	29.76	19.34	16.68	14.47	···
J_c (A/cm^3)	8.9×10^5	1.8×10^6	1.4×10^6	6.3×10^5	1.2×10^5	3.6×10^4	2.0×10^4	1.2×10^4	6.3×10^3	3.0×10^3	1.1×10^3	2.4×10^3	···

Here the $M\nearrow$ and $M\swarrow$ present the magnetization measured in the fields with positive and negative increments, respectively.
Sample No. 1293: size $\sim 1 \times 5 \times 2.08$ mm; mass $m = 0.0509$ g.

TABLE III. Comparison of the calculated J_c at 77 K from the nitric-treated sample with that previously made with a composition of $YBa_2Cu_{3.5}O_x$.

	J_c (A/cm^2) at field H (Tesla)					
Sample	0.05	0.1	0.5	1.0	3.0	4.0
No. 1281[a]	1.1×10^6	6.9×10^5	5.8×10^4	1.3×10^4	1.9×10^3	1.2×10^3
No. 5900[b]	···	5.8×10^4	···	9.0×10^2	6.0×10^2	6.0×10^2

[a]No. 1281: made by adding proportional CuO dissolved in HNO_3 into $YBa_2Cu_3O_x$ powder.
[b]No. 5900: prepared from a starting composition of $YBa_2Cu_{3.5}O_x$ powder as described in Ref. 1.

results for powder samples. We feel that the issue of the true circulating current size in such samples merits some attention.

Even with this ambiguity in the interpretation, we can quite clearly claim to have improved the properties in some way. How, depends partially upon the interpretation. For instance, it may be that the planar defects are good sites for trapping impurities that might otherwise collect at the grain boundaries. We believe that the difference in the microstructure is due to some solid solubility of copper (as planar defects) within the material. This contradicts conventional phase diagrams for the system, e.g.,[12] determined using x-ray diffraction techniques on powder samples. However, in a polycrystalline sample small planar defects are essentially invisible in an x-ray powder pattern, so there is room to question the details of the phase diagrams. It would appear to be very hard otherwise to explain their presence. It is relevant to mention that some recent (unpublished) results of our own indicate that in copper-rich samples annealed extensively at 860 °C excess copper does not phase separate; further work to look at this more closely is in progress.

ACKNOWLEDGMENT

This work was supported by the Science and Technology Center for Superconductivity on Grant No. NSF/DMR-8809854.

REFERENCES

1. J. P. Zhang, D. J. Li, L. D. Marks, C. H. Lin, J. A. Eades, A. Sodonis, W. Wolbach, J. M. Chabala, and R. Levi-Setti, J. Mater. Res. **7**, 572 (1992).
2. L. D. Marks, D. J. Li, H. Shibahara, and J. P. Zhang, J. Electron Microsc. Technique **8**, 297 (1988).
3. H. W. Zandbergen, R. Gronsky, K. Wang, and G. Thomas, Nature **331**, 596 (1988).

4. H. Shibahara, L. D. Marks, S-J. Hwu, and K. R. Poeppelmeier, J. Solid State Chem. **79**, 194 (1989).
5. R. Levi-Setti, Y. L. Wang, and G. Crow, Appl. Surf. Sci. **26**, 249 (1986).
6. J. M. Chabala, R. Levi-Setti, and Y. L. Wang, *Microbeam Analysis-1989* (San Francisco Press, San Francisco, CA, 1989), p. 586.
7. V. P. Dravid, H. Zhang, L. D. Marks, and J. P. Zhang, Physica C **192**, 31 (1992).
8. C. P. Bean, Phys. Rev. Lett. **8**, 250 (1962).
9. S. Jin, T. H. Tiefel, S. Nakahara, J. E. Graebner, H. M. O'Bryan, R. A. Fastnacht, and G. W. Kammlott, Appl. Phys. Lett. **56**, 1287 (1990).
10. S. T. Weir and W. J. Nellis, Appl. Phys. Lett. **56**, 2042 (1990).
11. D. C. Larbalestier, S. E. Babcock, X. Y. Cai, M. B. Field, Y. Gao, N. F. Heinig, D. L. Keiser, K. Merkle, L. K. Williams, and N. Zhang, Physica C **185**, 315 (1991).
12. R. N. Shelton, in *High Temperature Superconductivity,* edited by J. W. Lynn (Springer-Verlag, Berlin, 1990), p. 168.